AMERICAN SOCIETY FOR MICROBIOLOGY | Journal of Bacteriology®

MEETING PRESENTATION

Discovery of Calcium as a Biofilm-Promoting Signal for *Vibrio fischeri* Reveals New Phenotypes and Underlying Regulatory Complexity

Alice H. Tischler,[a] Louise Lie,[a] Cecilia M. Thompson,[a] Karen L. Visick[a]

[a]Loyola University Chicago, Maywood, Illinois, USA

ABSTRACT *Vibrio fischeri* uses biofilm formation to promote symbiotic colonization of its squid host, *Euprymna scolopes*. Control over biofilm formation is exerted at the level of transcription of the symbiosis polysaccharide (*syp*) locus by a complex set of two-component regulators. Biofilm formation can be induced by overproduction of the sensor kinase RscS, which requires the activities of the hybrid sensor kinase SypF and the response regulator SypG and is negatively regulated by the sensor kinase BinK. Here, we identify calcium as a signal that promotes biofilm formation by biofilm-competent strains under conditions in which biofilms are not typically observed (growth with shaking). This was true for RscS-overproducing cells as well as for strains in which only the negative regulator *binK* was deleted. The latter results provided, for the first time, an opportunity to induce and evaluate biofilm formation without regulator overexpression. Using these conditions, we determined that calcium induces both *syp*-dependent and bacterial cellulose synthesis (*bcs*)-dependent biofilms at the level of transcription of these loci. The calcium-induced biofilms were dependent on SypF, but SypF's Hpt domain was sufficient for biofilm formation. These data suggested the involvement of another sensor kinase(s) and led to the discovery that both RscS and a previously uncharacterized sensor kinase, HahK, functioned in this pathway. Together, the data presented here reveal both a new signal and biofilm phenotype produced by *V. fischeri* cells, the coordinate production of two polysaccharides involved in distinct biofilm behaviors, and a new regulator that contributes to control over these processes.

IMPORTANCE Biofilms, or communities of surface-attached microorganisms adherent via a matrix that typically includes polysaccharides, are highly resistant to environmental stresses and are thus problematic in the clinic and important to study. *Vibrio fischeri* forms biofilms to colonize its symbiotic host, making this organism useful for studying biofilms. Biofilm formation depends on the *syp* polysaccharide locus and its regulators. Here, we identify a signal, calcium, that induces both SYP-PS and cellulose-dependent biofilms. We also identify a new *syp* regulator, the sensor kinase HahK, and discover a mutant phenotype for the sensor kinase RscS. This work thus reveals a specific biofilm-inducing signal that coordinately controls two polysaccharides, identifies a new regulator, and clarifies the regulatory control over biofilm formation by *V. fischeri*.

KEYWORDS calcium, *Vibrio fischeri*, biofilms, calcium signaling, histidine kinase, sensor kinase, two-component regulatory systems

Biofilms are communities of microorganisms attached to surfaces and/or each other and are formed by bacteria in response to specific environmental signals (1–4). These signals can range from small molecules to physical surface detection and induce the production of biofilm matrices that contain a complex array of molecular compo-

Received 8 January 2018 **Accepted** 9 February 2018

Accepted manuscript posted online 20 February 2018

Citation Tischler AH, Lie L, Thompson CM, Visick KL. 2018. Discovery of calcium as a biofilm-promoting signal for *Vibrio fischeri* reveals new phenotypes and underlying regulatory complexity. J Bacteriol 200:e00016-18. https://doi.org/10.1128/JB.00016-18.

Editor George O'Toole, Geisel School of Medicine at Dartmouth

Address correspondence to Karen L. Visick, kvisick@luc.edu.

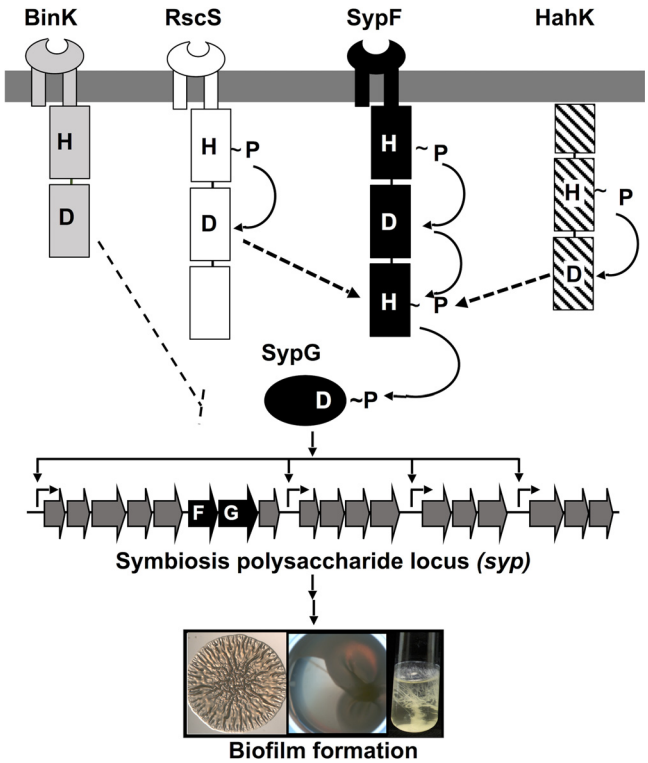

FIG 1 Model for the regulatory control over *syp*-dependent biofilm formation by *V. fischeri*. Previous work with plasmid-based overexpression of regulators revealed that the hybrid sensor kinase RscS induces biofilm formation in a manner that depends on the *syp* locus and the *syp* regulators SypF and SypG. The activity of RscS requires the indicated conserved residues (H412 and D709) in RscS as well as the conserved histidine (H705) within the last (Hpt) domain of SypF but not the conserved histidine (H250) or aspartate (D549) in the HisKA and REC domains of SypF (26, 32). SypF donates phosphoryl groups to both the response regulator SypG, the direct activator of the *syp* locus, and to the response regulator SypE (not shown), which controls *syp*-dependent biofilm formation at a level below *syp* transcription. BinK functions as a negative regulator of *syp*-dependent biofilm formation, at least in part due to the inhibition of *syp* transcription (33). This study confirms the position of RscS in the pathway and identifies HahK as another important sensor kinase whose activity feeds through the Hpt domain of SypF.

nents. Notably, polysaccharides are prominent matrix components that promote cell-cell and cell-surface attachment and contribute to protection from environmental stressors, such as antibiotics and host defense molecules (5–7).

Calcium is one small-molecule signal that controls biofilm formation in multiple bacterial species. Calcium affects biofilm formation through diverse mechanisms, either negatively (e.g., in *Staphylococcus aureus* [8] and *Vibrio cholerae* [9]) or positively (e.g., in *Xylella fastidiosa* [10], *Rhizobium leguminosarum* [11], *Pseudomonas aeruginosa* [12], and *Vibrio vulnificus* [13–15]). We recently demonstrated that salts, including calcium chloride, modestly impact biofilm formation by *Vibrio fischeri* (16). Specifically, calcium accelerates wrinkled colony formation, an indicator of biofilm formation (1).

For *V. fischeri*, biofilm formation is critical for colonization initiation of its symbiotic host, the Hawaiian bobtail squid *Euprymna scolopes* (reviewed in references 17–19). Two polysaccharide loci, the symbiosis polysaccharide (*syp*) locus and bacterial cellulose synthase (*bcs*) locus, are associated with biofilm formation (19–22) (Fig. 1; see also Fig. S1 in the supplemental material). The *syp* locus is an 18-gene locus that encodes glycosyltransferases and other proteins predicted to be involved in synthesis, modification, and export of SYP polysaccharide (SYP-PS) (23, 24). The *syp* genes are necessary for the production of SYP-PS, which promotes cell-cell interactions, while *bcs* encodes enzymes necessary for cellulose biosynthesis and appears to promote cell-surface interactions. *syp*-dependent biofilm formation by *V. fischeri* is well characterized; mutation of specific *syp* genes disrupts biofilm formation in culture as well as symbiotic biofilm formation (22, 23, 25–27).

Four two-component regulators control *syp*-dependent biofilm formation by *V. fischeri* (Fig. 1). Three regulators are encoded within the *syp* locus: SypG, a response regulator that serves as the direct transcriptional activator of *syp*; SypF, a sensor kinase that works upstream of SypG to control SYP-PS production; and SypE (not shown), a second response regulator that controls SYP-PS production at a level below *syp* transcription (21, 24, 26–29). The fourth regulator is a sensor kinase, RscS, encoded by an unlinked gene. The two sensor kinases, SypF and RscS, are both hybrid kinases with similar domain architecture, containing putative sensory and conserved domains predicted to be involved in autophosphorylation (HATPase/HisKA) and subsequent phosphorelay (REC and Hpt domains) (30, 31). A role for RscS in biofilm formation in culture has been observed only in the context of overexpression: overexpression of RscS is sufficient to induce SYP-PS production and biofilm formation, as seen by the production of cohesive wrinkled colonies on solid medium, the formation of pellicles in static liquid medium, and enhanced symbiotic biofilms (22). These RscS-induced biofilms require SypF (26). Biofilm formation can be restored through complementation with the Hpt domain of SypF alone. As the Hpt domain of RscS is not essential for its activity (32), distinct domains within the two proteins, RscS and SypF, appear to work together to drive the signal transduction necessary for *syp* transcription and biofilm formation.

Recently, the involvement of a third sensor kinase, BinK, was reported (33, 34). BinK inhibits the production of *syp*-dependent biofilms induced by RscS overexpression, and loss of BinK enhances symbiotic biofilm formation and colonization (Fig. 1). The inhibitory effect of BinK occurs, at least in part, at the level of *syp* transcription, as disruption of *binK* increased expression of a *syp* reporter fusion. The mechanism of how BinK interfaces with other Syp regulatory proteins and exerts its effect on *syp* transcription remains unknown.

Here, we report the discovery that calcium supplementation induced the production of biofilms. These calcium-induced phenotypes were dependent on both the *syp* and *bcs* loci, indicating coordinate production of these two polysaccharides. Moreover, we determined that a single mutation, disrupting the negative regulator *binK*, was sufficient for *V. fischeri* to produce biofilms in response to calcium. This finding is significant because it permitted assessment of biofilm regulation in culture in the absence of overexpression of positive biofilm regulators. As a result, we uncovered the involvement of a new *syp* regulator, HahK, and identified, for the first time, a mutant phenotype in culture for the known *syp* regulator RscS.

RESULTS

Calcium induces biofilm formation. Previous work indicated that calcium accelerates wrinkled colony formation by *V. fischeri* (16). To further explore the importance of calcium in biofilm formation, we assayed a number of strains under a variety of growth conditions in which calcium was added to the rich growth medium LBS. In many cases, the impact of calcium was modest. For example, calcium addition to plates promoted subtle changes in wrinkled colony formation by strain KV7655, which contains a second chromosomal copy of the gene for the positive biofilm regulator RscS (*rscS*$^{++}$) (Table 1), and, as seen previously (16), some slight amount of colony architecture by wild-type strain ES114 relative to that in the absence of calcium (Fig. 2A). In other cases, however, the impact was striking: the same *rscS*$^{++}$ strain (KV7655) produced robust pellicles in static liquid culture only in the presence of calcium (Fig. 2B, note cohesive biofilm, indicated by an arrow). Furthermore, we found that calcium could induce biofilm phenotypes under conditions that are not typically permissive for biofilm formation, namely, shaking liquid (LBS) cultures. While ES114 grows as a fully turbid culture in the presence of calcium under these conditions, the *rscS*$^{++}$ strain exhibited two distinct biofilm phenotypes: a ring around the test tube surface above the top of the liquid (in the "splash zone") and a cohesive cellular clump at the bottom of the tube (Fig. 2C). These biofilm phenotypes were specific to calcium and not induced by supplementation with other cations (Fig. 2D). Calcium also induced clump and ring formation by other biofilm-competent strains, including strains over-

TABLE 1 Strains used in this study

Strain	Genotype[a]	Derivation[b]	Reference or source
ES114	Wild type		51
KV712	Rif^r *rscS*::Tn*10-lacZ*		39
KV1787	Δ*sypG*		71
KV4567	attTn*7*::P*bcsQ-lacZ*	Derived from ES114 using pCMA26	This study
KV4607	Δ*binA bcsA*::Tn*5*		20
KV5097	Δ*sypK*		65
KV5367	Δ*sypF*		26
KV6533	Δ*rscS*	Derived from ES114 using pKV456 (26)	This study
KV7371	IG (*yeiR-glmS*)::P*sypA-lacZ*		26
KV7410	IG (yeiR-glmS)::P*sypA-lacZ* attTn*7*::Em		26
KV7655	attTn*7*::*rscS*	Derived from ES114 using pANN78 (26)	This study
KV7860	Δ*binK*	Derived from ES114 using pLL2	This study
KV7861	Δ*binK* Δ*rscS*	Derived from KV6533 using pLL2	This study
KV7862	Δ*binK* Δ*sypF*	Derived from KV5367 using pLL2	This study
KV7871	Δ*sypF* Δ*binK* attTn*7*::*sypF*-Hpt-H705Q-FLAG	Derived from KV7862 using pANN58 (26)	This study
KV7873	Δ*sypF* Δ*binK* attTn*7*::*sypF*-H705Q-FLAG	Derived from KV7862 using pANN45 (26)	This study
KV7875	Δ*sypF* Δ*binK* attTn*7*::*sypF*-H250Q-FLAG	Derived from KV7862 using pANN24 (26)	This study
KV7877	Δ*sypF* Δ*binK* attTn*7*::*sypF*-Hpt-FLAG	Derived from KV7862 using pANN50 (26)	This study
KV7878	Δ*sypF* Δ*binK* attTn*7*::*sypF*-FLAG	Derived from KV7862 using pANN20 (26)	This study
KV7879	Δ*sypF* Δ*binK* attTn*7*::*sypF*-D549A-FLAG	Derived from KV7862 using pANN21 (26)	This study
KV7894	Δ*bcsA*	Derived from ES114 using pKPQ22 (72)	This study
KV7906	Δ*binK* Δ*sypK*	Derived from KV5097 using pLL2	This study
KV7908	Δ*binK* Δ*bcsA*	Derived from KV7894 using pLL2	This study
KV7914	Δ*binK* Δ*sypK* Δ*bcsA*	Derived from KV7906 using pKPQ22 (72)	This study
KV7933	Δ*binK* Δ*sypG*	Derived from KV1787 using pLL2	This study
KV7937	Δ*sypF* Δ*binK rscs*::Tn*10*	NT of KV7862 with cKV712	This study
KV7949	Δ*sypF* Δ*binK rscs*::Tn*10* attTn7::*sypF*-HPT	Derived from KV7937 using pANN50 (26)	This study
KV8037	Δ*binK* attTn*7*::P*bcsQ-lacZ*	NT of KV7860 with cKV4567	This study
KV8038	Δ*binK* IG (*yeiR-glmS*)::P*sypA-lacZ* attTn*7*::Em	NT of KV7860 with cKV7410	This study
KV8069	Δ*sypQ*::Cm	NT of ES114 using PCR DNA generated with primers 443, 2174, 2089, 2090, 1188, and 2175	This study
KV8076	Δ*binK* Δ*sypQ*::Cm attTn*7*::P*bcsQ-lacZ*	NT of KV8037 with cKV8069	This study
KV8077	Δ*binK* Δ*sypQ*::Cm IG (*yeiR-glmS*)::P*sypA-lacZ* attTn*7*::Em	NT of KV8038 with cKV8069	This study
KV8078	Δ*sypQ*::Cm attTn*7*::P*bcsQ-lacZ*	NT of KV4567 with cKV8069	This study
KV8079	Δ*sypQ*::Cm IG (*yeiR-glmS*)::P*sypA-lacZ* attTn*7*::Em	NT of KV7410 with cKV8069	This study
KV8297	Δ*hahK*::FRT-Trim IG (yeiR-glmS)::*laclq*	NT of KV6576 (73) with PCR DNA generated from primers 2057, 2103, 2089, 2090, 2062, and 2104	This study
KV8323	Δ*sypF* Δ*binK* Δ*hahK*::FRT-Trim attTn7::*sypF*-Hpt-FLAG	NT of KV7877 with cKV8297	This study
KV8324	Δ*sypF* Δ*binK* Δ*hahK*::FRT-Trim attTn7::*sypF*-FLAG	NT of KV7878 with cKV8297	This study
KV8325	Δ*sypF* Δ*binK* Δ*hahK*::FRT-Trim *rscS*::Tn*10* attTn7::*sypF*-Hpt-FLAG	NT of KV7949 with cKV8297	This study

[a]Abbreviations: FLAG, FLAG epitope tagged; IG (*yeiR-glmS*), intergenic between *yeiR* and *glmS* (adjacent to the Tn*7* site); FRT, the Em^r or Cm^r cassette was resolved using Flp recombinase, leaving a single FRT sequence.

[b]Derivation of strains constructed in this study. NT, natural transformation of a pLostfoX- or pLostfoX-Kan-carrying version of the indicated strain with the indicated chromosomal (c) DNA or with a PCR-SOE product generated using the indicated primers and, as templates, ES114 and either an Em^r or Cm^r cassette.

expressing *rscS* from a multicopy plasmid or overexpressing positive regulator *sypG* in the absence of the negative regulator *sypE* (Table 2; see Fig. S2 in the supplemental material). For these plasmid-containing biofilm-competent strains, the ring-and-clump phenotypes were less robust than those seen for *rscS*$^{++}$, potentially due to the necessary addition of antibiotics for plasmid maintenance. Together, these data indicate that calcium is a strong inducer of biofilms, as it specifically triggers *V. fischeri* to form biofilms under classically nonpermissive conditions (i.e., shaking liquid cultures). These calcium-induced shaking liquid phenotypes also provide a novel phenotype to study regulatory pathways in *V. fischeri* biofilm formation.

BinK inhibits calcium-induced biofilm formation. Another strain that we examined was a strain deleted for the negative regulator *binK*. The report that identified BinK had examined its role in the context of *rscS* overexpression. It showed that disruption of *binK* accelerated the onset of wrinkled colony formation when *rscS* was overexpressed, and that *binK* overexpression inhibited RscS-induced wrinkled colonies, result-

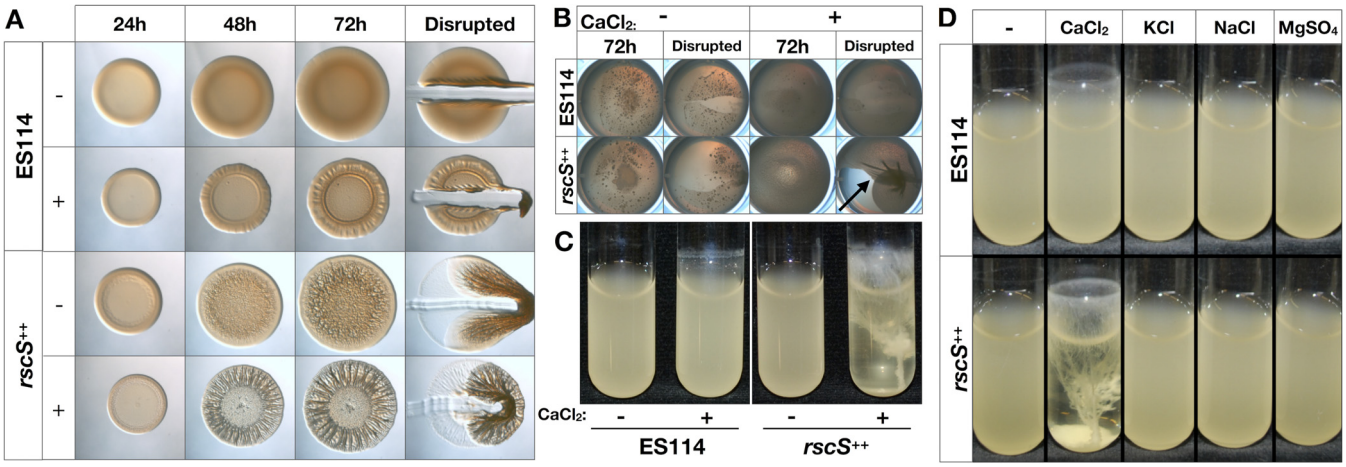

FIG 2 Calcium induces biofilm formation. Biofilm formation was assessed for wild-type *V. fischeri* (ES114) and *rscS*$^{++}$ (KV7655) strains. (A) Wrinkled colony formation was assessed by a time course on LBS agar plates lacking or containing 10 mM $CaCl_2$ as indicated. Colonies were disrupted at the final time point to evaluate SYP-PS production. (B) Pellicle formation was assessed at 72 h after static incubation in LBS either lacking or containing 10 mM $CaCl_2$, as indicated. Pellicles were disrupted to determine cohesiveness. The arrow indicates a cohesive pellicle. (C) ES114 and *rscS*$^{++}$ strains were grown in LBS medium, with shaking, either lacking or containing 10 mM $CaCl_2$. (D) ES114 and *rscS*$^{++}$ strains were grown in LBS medium alone or medium supplemented with 10 mM $CaCl_2$, KCl, NaCl, or $MgSO_4$, as indicated.

ing in smooth colonies (33). Given that both *binK* and calcium affect wrinkling of biofilm-competent strains, we hypothesized that loss of BinK would enhance calcium-dependent biofilm formation. We further hypothesized that the loss of this negative regulator alone would be sufficient to permit biofilm formation in the presence of calcium. We thus evaluated the biofilm phenotypes of a Δ*binK* mutant using our three assays, the formation of wrinkled colonies, pellicles, and rings/clumps. In the absence of calcium, the *binK* mutant did not produce any visible biofilms (Fig. 3A to C). However, when calcium was added, the *binK* mutant formed robust biofilms under all three conditions (Fig. 3A to C). As with the *rscS*$^{++}$ strain, the ring/clump formation was

TABLE 2 Plasmids used in this study

Plasmid	Characteristics[a]	Reference or source
pANN20	pEVS107 + *sypF*-FLAG	26
pANN21	pEVS107 + *sypF*-D549A-FLAG	26
pANN24	pEVS107 + *sypF*-H250Q-FLAG	26
pANN45	pEVS107 + *sypF*-H705Q-FLAG	26
pANN50	pEVS107 + *sypF*-Hpt-FLAG	26
pANN58	pEVS107 + *sypF*-Hpt-H705Q-FLAG	26
pANN78	pEVS107 + *rscS*	26
pCLD51	pTMO82 containing P*bcsQ*, generated using primers 835 and 836	This study
pCMA26	pEVS107 containing P*bcsQ-lacZ* reporter from pCLD51	This study
pCP20	Encodes *flp* recombinase	69
pEVS107	Vector for delivery of DNA into the Tn*7* site, Km^r Em^r	66
pKPQ22	pKV363 plus sequences flanking *bcsA* to generate *bcsA* deletion	72
pKV363	Suicide vector, Cm^r	65
pKV456	pKV363 plus sequences flanking *rscS*	26
pLL2	pKV363 plus sequences flanking *binK*, generated with primers 1268, 1269, 1270, and 1271, to generate *binK* deletion	This study
pLostfoX	Vector for *tfoX* expression for natural transformation, Cm^r	56
pLostfoX-Kan	Vector for *tfoX* expression for natural transformation, Km^r	57
pTMO82	Vector containing promoterless *lacZ* gene, Km^r Ap^r	25
pUX-BF13	Delivery plasmid for Tn*7* transposase	68

[a]Details on construction are included for plasmids generated in this study; ES114 was used as the template for PCRs.

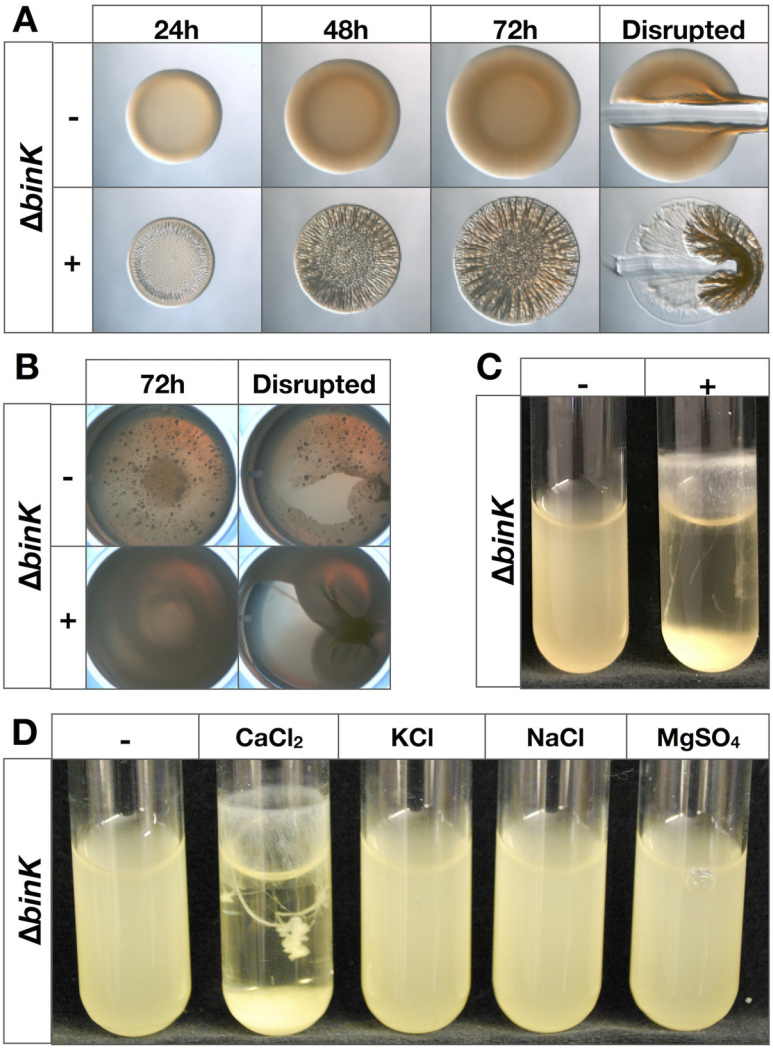

FIG 3 Calcium induces biofilm formation by a *binK* mutant. Biofilm formation was assessed for the *V. fischeri* Δ*binK* (KV7860) strain. (A) Wrinkled colony formation was assessed by a time course on LBS agar plates lacking or containing 10 mM $CaCl_2$, as indicated. Colonies were disrupted at the final time point to evaluate SYP-PS production. (B) Pellicle formation was assessed at 72 h after static incubation in LBS either lacking or containing 10 mM $CaCl_2$ as indicated. Pellicles were disrupted to determine cohesiveness. (C) Δ*binK* strain was grown in LBS medium, with shaking, either lacking or containing 10 mM $CaCl_2$. (D) Δ*binK* strain was grown in LBS medium, with shaking, either lacking or containing 10 mM $CaCl_2$. (D) ES114 and *rscS*$^{++}$ strains were grown in LBS medium alone or medium supplemented with 10 mM $CaCl_2$, KCl, NaCl, or $MgSO_4$, as indicated.

specific to calcium (Fig. 3D). These data reveal BinK as a strong negative regulator that alone is sufficient to suppress calcium-dependent biofilm formation in *V. fischeri*. Additionally, this simple combination of genetic (*binK* disruption) and environmental (calcium supplementation) conditions is sufficient to overcome the need for overexpression of positive regulators to induce *in vitro* biofilm formation.

Calcium-induced rings and clumps form separately. Because the rings and clumps produced in culture in response to calcium appeared as distinct phenotypes, we visually evaluated their development over time using the *binK* mutant. We found that ring formation occurred as early as 2 to 4 h after inoculation of a single colony into broth containing calcium (Fig. S3), while clumping occurred later (around 11 h in the experiment shown in Fig. 4). The two biofilms progressed over time, with the rings often developing tendrils that merged with/attached to the cellular clumps. The distinct timing and position of these biofilms suggested that discrete processes are involved in their growth and maturation.

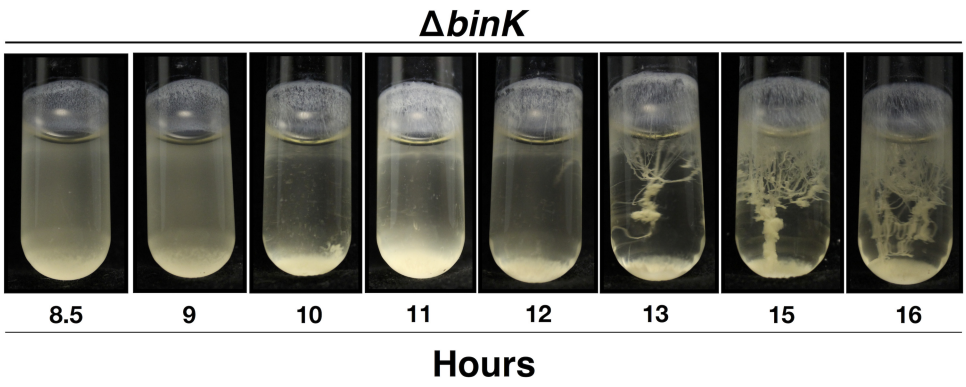

FIG 4 Calcium-induced rings and clumps form separately. Biofilm phenotypes of the Δ*binK* (KV7860) strain, supplemented with 10 mM $CaCl_2$, were evaluated over time using multiple cultures grown from single colonies. The independent cultures behaved similarly. Representative images from different tubes were captured at the indicated times postinoculation.

Calcium-induced biofilms are *syp* and *bcs* dependent. Since RscS and BinK both control *syp* transcription and *syp*-dependent wrinkled colony formation (33), we hypothesized that disruption of *syp* would abolish calcium-induced liquid biofilms. Deletion of most of the 18 *syp* genes eliminate wrinkled colony formation and pellicle production (23), so a representative gene, *sypK*, was chosen to assess the role of *syp* in the shaking biofilm phenotypes. Deletion of *sypK* abolished production of the cohesive cellular clump, but not ring formation, by the *binK* mutant (Fig. 5A). We quantified this effect by staining the biofilm material with crystal violet (Fig. 5A, middle) and then solubilizing and measuring the stain (Fig. 5A, bottom). The amount of biofilm produced by the *binK sypK* double mutant was significantly less than that produced by the *binK* mutant alone. We thus conclude that cell clumping requires an intact *syp* locus.

Since disruption of *syp* had no impact on ring formation, we hypothesized that another polysaccharide locus, such as the cellulose locus (20), is responsible for ring production. To test this hypothesis, we asked if deletion of *bcsA*, which encodes a subunit of cellulose synthase, abolished ring formation. A *binK bcsA* double mutant failed to form rings, indicating that ring formation requires an intact cellulose locus. This double mutant retained the ability to produce cohesive cellular clumps and produced substantially less polysaccharide than the single *binK* mutant alone (Fig. 5A).

These data suggested that both SYP and cellulose polysaccharides contribute to the biofilm phenotypes observed under these conditions. Indeed, disrupting both *syp* and *bcs* (Δ*binK* Δ*sypK* Δ*bcsA*) prevented production of both rings and clumps by the *binK* mutant (Fig. 5A). In fact, the phenotype of the triple mutant was similar to that of cultures grown in the absence of calcium (Fig. 5A). Each of the two phenotypes could be restored separately to the triple mutant by complementation with the appropriate *syp* or *bcs* gene (Fig. S4A and B). In addition, we observed similar biofilm defects when we assayed *syp* and *bcs* mutants in an RscS-overexpressing strain (Fig. S4C). Thus, SYP-PS and cellulose are both required for liquid biofilm formation, and disruption of *binK* largely phenocopies overexpression of RscS under these conditions.

Calcium induces two distinct polysaccharide biofilms in liquid culture, but for wrinkled colonies, only SYP-PS is known to be important, as disruption of *syp* results in smooth colonies in the context of RscS overexpression (23, 24). We therefore investigated whether both SYP-PS and cellulose were important for calcium-induced wrinkled colony formation. A *binK sypK* double mutant failed to form wrinkles or cohesive colonies in the presence of calcium, suggesting that SYP-PS is necessary for colony architecture and cohesion (Fig. 5B). Conversely, a *binK bscA* double mutant formed colonies phenotypically indistinguishable from a *binK* mutant in the presence of calcium, while the triple *binK sypK bcsA* mutant was smooth (Fig. 5B). Thus, robust wrinkling and cohesive colonies require only SYP-PS and not cellulose.

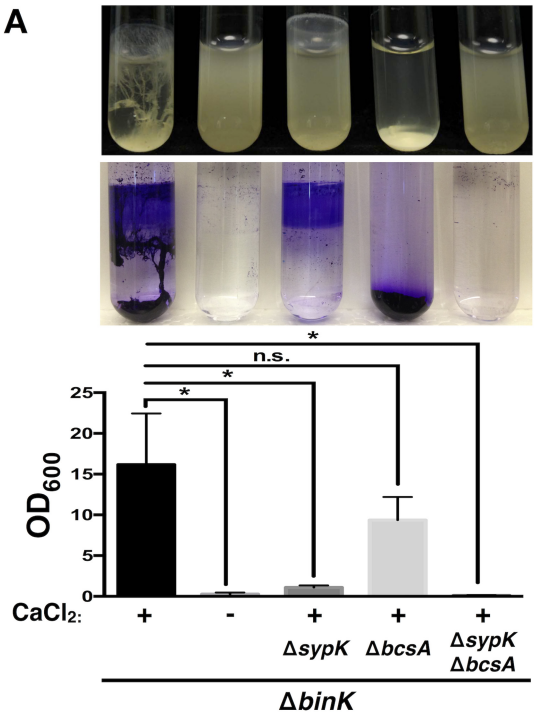

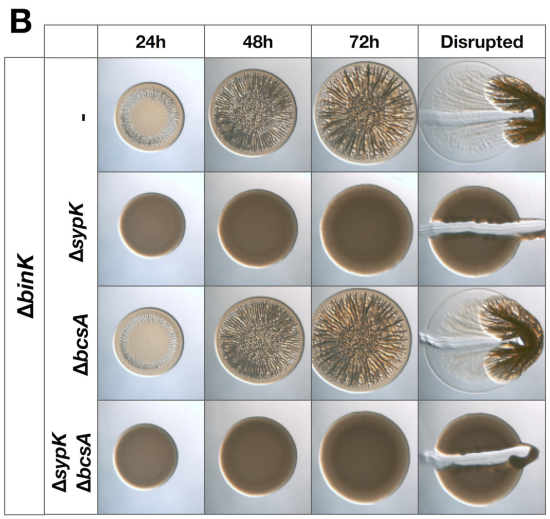

FIG 5 Calcium-induced biofilms are *syp* and *bcs* dependent. The contribution of specific polysaccharides to calcium-induced *V. fischeri* biofilms was evaluated using Δ*binK* (KV7860), Δ*binK* Δ*sypK* (KV7906), Δ*binK* Δ*bcsA* (KV7908), and Δ*binK* Δ*sypK* Δ*bcsA* (KV7914) strains. (A, top) Strains were grown shaking in LBS medium either lacking or containing 10 mM $CaCl_2$, as indicated, and imaged 16 h postinoculation. (Middle) Tubes were stained with crystal violet and imaged. (Bottom) Crystal violet was quantified, and a one-way ANOVA was performed (*P* values of 0.01, 0.01, 0.1 [not significant {n.s.}], and 0.01). (B) Wrinkled colony formation was assessed by a time course on LBS agar plates lacking or containing 10 mM $CaCl_2$, as indicated. Colonies were disrupted at the final time point to evaluate SYP-PS production.

Calcium impacts transcription of *syp* and *bcs*. Given that calcium induces liquid biofilm phenotypes that depend on two distinct polysaccharides, we hypothesized that this effect occurs at the level of transcription of the *bcs* and *syp* polysaccharide loci. Transcriptional reporters for the promoter regions of *bcsQ* and *sypA* revealed a significant increase in transcription of both promoters in the presence of calcium (Fig. 6). This calcium-dependent increase was more substantial at both promoters in a *binK* mutant, especially at the *sypA* promoter (Fig. 6). The effect of *binK* disruption on *syp* and *bcs* transcription is consistent with recent reports (33, 34). These data suggest that (i)

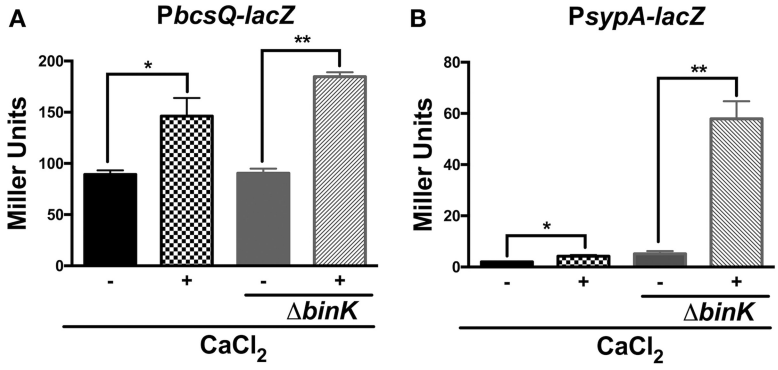

FIG 6 Calcium induces *syp* and *bcs* transcription. Transcription of the *bcs* and *syp* genes was assessed using a promoterless *lacZ* reporter gene fused to the promoter regions of *bcsQ* (A) and *sypA* (B). *V. fischeri* cells were grown at 24°C with shaking in 20 ml of LBS supplemented, as indicated, with 10 mM $CaCl_2$. (A) The effect of calcium on *bcsQ* transcription was monitored using P_{bcsQ}-*lacZ* (KV8078) ($P = 0.02$) and Δ*binK* P_{bcsQ}-*lacZ* (KV8076) ($P = 0.0025$) strains. (B) The effect of calcium on *sypA* transcription was monitored using P_{sypA}-*lacZ* (KV8079) ($P = 0.03$) and Δ*binK* P_{sypA}-*lacZ* (KV8077) ($P = 0.004$) strains.

calcium promotes biofilm formation, at least in part, by inducing transcription of *bcs* and *syp* loci and (ii) BinK inhibits the effect of calcium on transcription of both loci.

Calcium-dependent cell clumping depends on *sypF* and *sypG*. The identification of new phenotypes and conditions that induce biofilm formation in the absence of overexpression of regulators provided an opportunity to reassess the roles of known *syp* regulators. We thus asked if SypF, SypG, and/or RscS were required for calcium-dependent biofilm formation (Fig. 1). We generated double deletion mutants and assessed cell clumping in shaking cultures and wrinkled colony formation on plates. All of the mutants retained the ability to form rings, but the *binK sypF* and *binK sypG* mutants produced turbid instead of clumped cultures. Visual observation of these cultures and subsequently of the crystal violet-stained tubes confirmed that the double mutants formed substantially less biofilm than a single *binK* mutant (Fig. 7A). The *binK sypF* and *binK sypG* mutants generated smooth, noncohesive colonies, unlike the fully wrinkled and cohesive *binK* mutant (Fig. 7B). These results indicate the importance of these regulators in wrinkling and cell clumping but not ring formation. In contrast, the phenotype of a *binK rscS* mutant was indistinguishable from that of the *binK* single mutant (Fig. 7). Therefore, despite RscS's clear positive contribution to biofilm formation (Fig. 2 and Fig. S2) (22), it does not seem to be required for biofilm formation in the absence of BinK; similarly, *binK* disruption is not required when RscS is overexpressed (Fig. 2). These data indicate that the calcium-dependent cell clumping and wrinkled colony formation that occur under these conditions in the absence of *binK* require *sypF* and *sypG* but not *rscS*.

The Hpt domain of SypF is sufficient for calcium-dependent cell clumping. When RscS is overexpressed, only the Hpt domain of SypF is necessary for biofilm formation (Fig. 1) (26). Since SypF, but not RscS, is necessary for biofilms in a *binK* mutant (Fig. 7), we wondered whether full-length SypF was required or if only a specific domain would be sufficient for calcium-induced, *syp*-dependent cell clumping. We thus introduced, into the double *binK sypF* mutant, various *sypF* alleles that encode proteins with substitutions in residues predicted to be involved in the phosphorelay, H250Q, D549A, and H705Q, as well as expressing the Hpt domain alone (Fig. 1). Consistent with our previous work (26), expression of wild-type SypF, SypF-H250Q, and SypF-D549A each restored cell clumping to the *binK sypF* mutant (Fig. 8). Expression of the Hpt domain alone was similarly able to restore clumping, while the Hpt domain with a H705Q mutation resulted in a significant and complete loss of cell clumping (Fig. 8). These data indicate that a phosphorylatable Hpt domain is the only domain of SypF necessary for BinK-inhibited, calcium-dependent cell clumping.

The sensor kinase HahK promotes cell clumping and colony wrinkling. As autophosphorylation activity of SypF is not required for calcium-dependent cell clump-

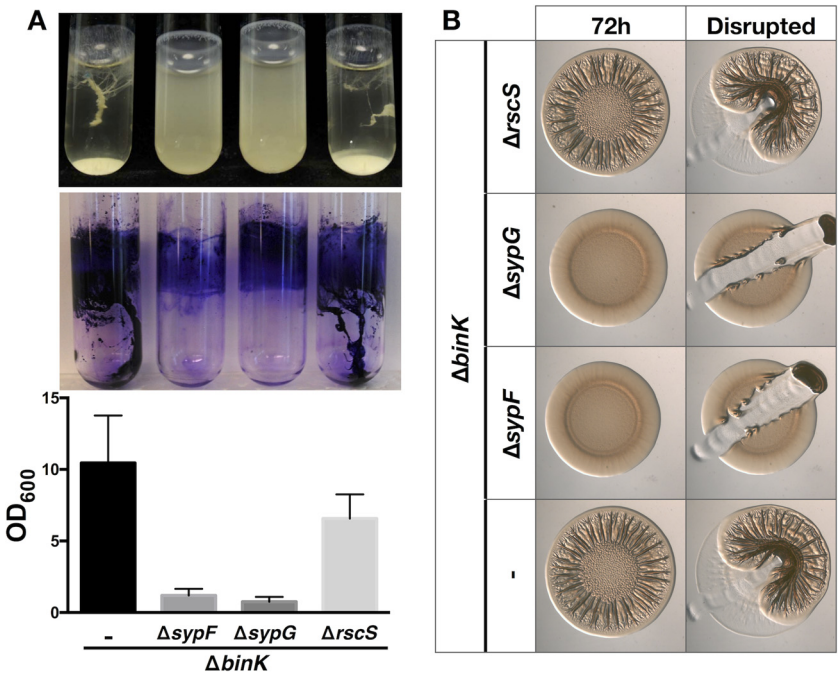

FIG 7 Calcium-dependent cell clumping depends on *sypF* and *sypG*. The contribution of SypF, SypG, and RscS to calcium-induced *V. fischeri* biofilms was evaluated in Δ*binK* (KV7860), Δ*binK* Δ*sypF* (KV7862), Δ*binK* Δ*sypG* (KV7933), and Δ*binK* Δ*rscS* (KV7861) strains. (A, top) Strains were grown shaking in LBS medium supplemented with 10 mM $CaCl_2$ and imaged 16 h postinoculation. (Middle) Tubes were stained with crystal violet and imaged. (Bottom) Crystal violet was quantified, and a one-way ANOVA was performed (*P* values of 0.09, 0.07, and 0.5 compared to KV7860). (B) Wrinkled colony formation was assessed by incubation for 72 h on LBS agar plates containing 10 mM $CaCl_2$. Colonies were disrupted to evaluate SYP-PS production.

ing (Fig. 8), the Hpt domain of SypF must become phosphorylated by another mechanism. We considered the involvement of another sensor kinase. Specifically, we looked for genes in the *V. fischeri* genome that encoded a sensor kinase with the right domain structure (poised to donate a phosphoryl group to the Hpt domain of SypF via a REC domain) and were unlinked to genes for putative DNA-binding response regulators. Because biofilm formation is an important colonization determinant, we prioritized those sensor kinases that appeared important for symbiotic colonization (33). As a result, we focused our attention on four possible uncharacterized regulators, *VF_2379*, *VF_1296*, *VF_1053*, and *VF_A0072*. Of these, only deletion of *VF_A0072* had any effect on calcium-induced biofilm formation by the *binK* mutant, although the effect was subtle, with only a delay but not loss of biofilm formation (Fig. S5). VF_A0072 is a cytoplasmic sensor kinase with HTPase, HisKA, and REC domains (Fig. 1). Although it is uncharacterized, its gene has previously been named *hahK* (HnoX-associated histidine kinase gene) due to its location within an operon downstream of the gene for HnoX, a nitric oxide sensor (35, 36). For simplicity and consistency, we will refer to *VF_A0072* as *hahK*.

We hypothesized that, when SypF is intact, it is capable of promoting calcium-induced biofilm formation independent of *hahK* and that the role of HahK, if any, would be more apparent when only the Hpt domain of SypF was present. Therefore, we generated a strain deleted for *binK*, *sypF*, and *hahK* and then introduced *sypF*-Hpt into the chromosome. Biofilm formation by this strain was assessed using the cell clumping and wrinkled colony assays. While the Δ*binK sypF-Hpt* control strain was competent to produce cell clumps in response to calcium, the equivalent strain that lacked HahK formed significantly less biofilm and very small clumps (Fig. 9A). In contrast, when full-length *sypF* was restored to the *binK sypF hahK* mutant, an intermediate phenotype was observed, as the cells clumped but overall biofilm formation was significantly reduced (Fig. 9A). These phenotypes were mirrored on plates as the Δ*binK sypF-Hpt*

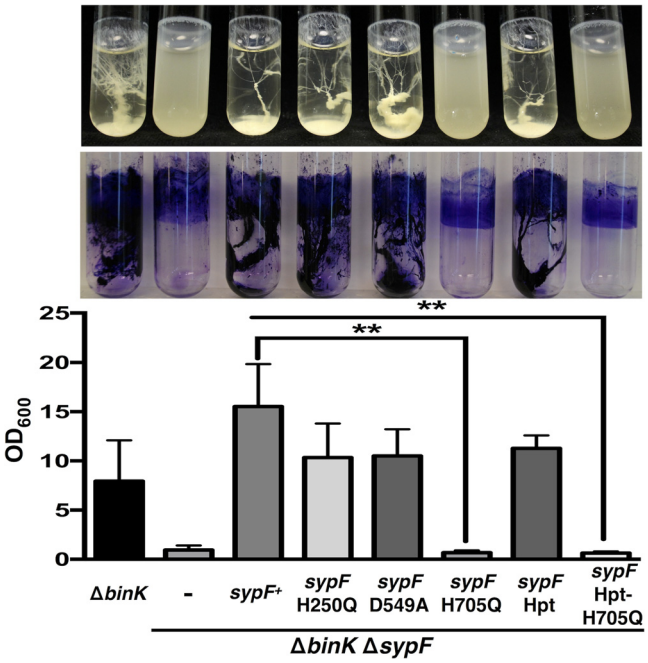

FIG 8 Hpt domain of SypF is required for calcium-induced clumps. The requirement for specific SypF residues and domains in calcium-induced *V. fischeri* biofilm formation was evaluated. (Top) Strains were grown shaking in LBS medium containing 10 mM $CaCl_2$ and imaged 16 h postinoculation. (Middle) Tubes were stained with crystal violet and imaged. (Bottom) Crystal violet was quantified, and a one-way ANOVA was performed (*P* values were not significant [ns], 0.004, ns, and 0.004). Strains, from left to right, are the Δ*binK* (KV7860), Δ*binK* Δ*sypF* (KV7862), Δ*binK* Δ*sypF sypF*$^+$ (KV7878), Δ*binK* Δ*sypF sypF-H250Q* (KV7875), Δ*binK* Δ*sypF sypF-D549A* (KV7879), Δ*binK* Δ*sypF sypF-H705Q* (KV7873), Δ*binK* Δ*sypF sypF-HPT* (KV7877), and Δ*binK* Δ*sypF sypF-HPT-H705Q* (KV7871) strains.

mutant was cohesive and wrinkled, while the mutant lacking HahK had only minimal wrinkling and slight cohesiveness (Fig. 9B). Similar to the liquid phenotype, the wrinkled colony assay showed an intermediate phenotype for the HahK mutant in the context of a full-length SypF: this strain had a slight amount of architecture and retained cohesiveness (Fig. 9B). The triple mutant expressing SypF-Hpt was complemented by a plasmid overexpressing *hahK* (Fig. S6). Together, these data indicate that HahK is an active member of this pathway, potentially by acting through the Hpt domain of SypF (Fig. 1).

RscS contributes to calcium-dependent biofilms. Loss of *hahK* severely diminishes, but does not fully abolish, polysaccharide production (Fig. 9), so we hypothesized that a third sensor kinase is working through SypF-Hpt to promote SYP-PS. RscS was considered a candidate for this sensor kinase, as it has previously been shown to work through the Hpt domain of SypF (26). To test this possibility, we first constructed an *rscS* mutation in the *binK sypF*-Hpt mutant background and assessed its ability to form calcium-induced biofilms. In liquid culture, these mutants were virtually indistinguishable from the control strain, similar to what we observed previously in the context of a *binK* mutation alone (Fig. 6 and 10A). Additionally, wrinkled colony formation of the *rscS* mutant strain was only slightly delayed compared to that of the control strain, with the control strain showing increased architecture at 30 h (Fig. 10B). If SypF, HahK, and RscS all work through the Hpt domain of SypF, then the presence of HahK in these strains may be obscuring the contribution of RscS. To test this hypothesis, we constructed a strain with mutations in both *rscS* and *hahK* (in the background of a *binK sypF-Hpt* strain) and assessed calcium-dependent biofilm formation. Biofilm formation was significantly decreased in these strains compared to that of the control, with cell clumping completely abrogated and ring formation substantially diminished (Fig. 10A). On solid agar, colonies were completely smooth, with no detectable cohesiveness

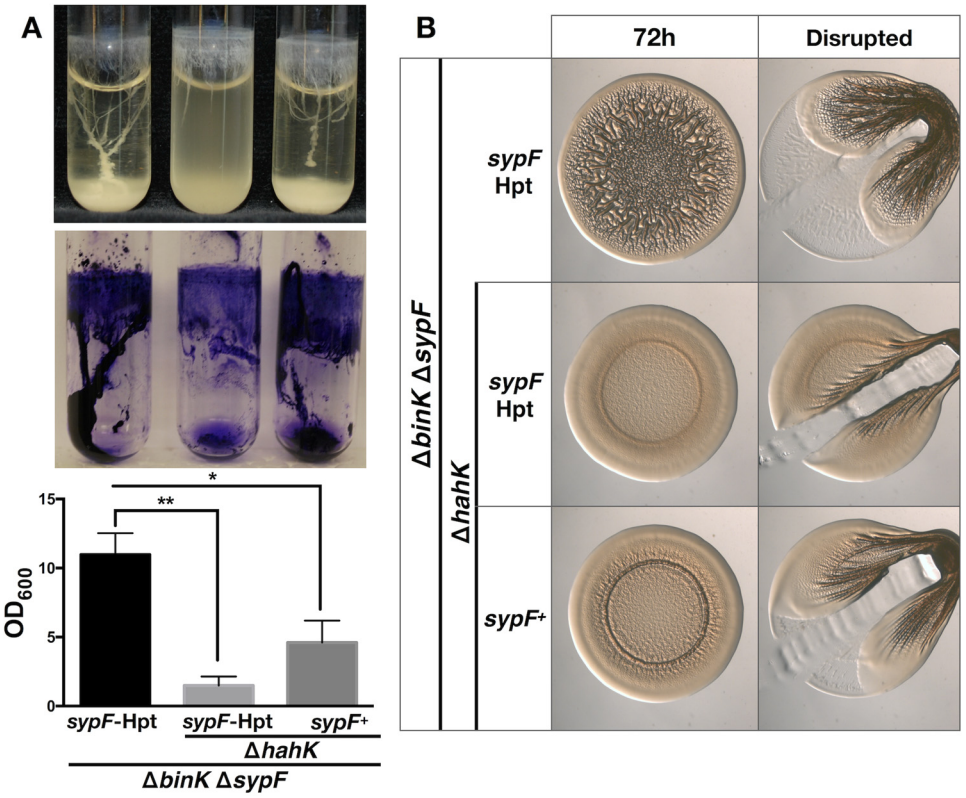

FIG 9 Sensor kinase HahK promotes cell clumping and colony wrinkling. The contribution of *hahK* to calcium-induced *V. fischeri* biofilms was evaluated in Δ*binK* Δ*sypF sypF-HPT* (KV7877), Δ*binK* Δ*sypF* Δ*hahK sypF-HPT* (KV8323), and Δ*binK* Δ*sypF* Δ*hahK sypF*$^+$ (KV8324) strains. (A, top) The strains were grown shaking in LBS medium containing 10 mM $CaCl_2$ and imaged 16 h postinoculation. (Middle) Tubes were stained with crystal violet and imaged. (Bottom) Crystal violet was quantified and a one-way ANOVA was performed (*P* values of 0.002 and 0.03). (B) Wrinkled colony formation was assessed by incubation for 72 h on LBS agar plates containing 10 mM $CaCl_2$. Colonies were disrupted to evaluate SYP-PS.

when disrupted (Fig. 10B). The loss of both *rscS* and *hahK* could be complemented by a plasmid expressing either RscS or HahK (Fig. S7). These data support a role for RscS in calcium-dependent cell clumping and wrinkled colony formation that was previously obscured by multiple sensor kinase inputs. This marks the first mutant phenotype in culture for *rscS* since its discovery and highlights the complexity and redundancy of regulators in the control of *V. fischeri* biofilm formation.

DISCUSSION

Wild-type *V. fischeri* naturally forms a biofilm during colonization of its symbiotic squid host, yet it forms biofilms poorly under standard laboratory conditions (22, 37). Substantial biofilm development has only been detected previously when positive regulators, such as RscS or SypG, are overexpressed. These overexpression conditions have been extremely fruitful in identifying the contributions made by positive and negative factors, including specific proteins encoded by the *syp* locus (e.g., see references 22, 23, 27, and 38) and BinK (33). However, the use of overexpression conditions can limit the scope of our understanding by bypassing natural regulatory processes. Here, we report new conditions that obviate overexpression of positive regulators to promote *in vitro* biofilm formation by *V. fischeri*. These new conditions have permitted a deeper understanding of biofilm regulation and have facilitated the identification of a new regulator in the control over biofilm by *V. fischeri*.

Specifically, we have identified calcium as a major regulator of biofilm formation. This requirement had not been apparent in previous work that depended on the overexpression of positive regulators of biofilm formation, such as RscS, as these strains

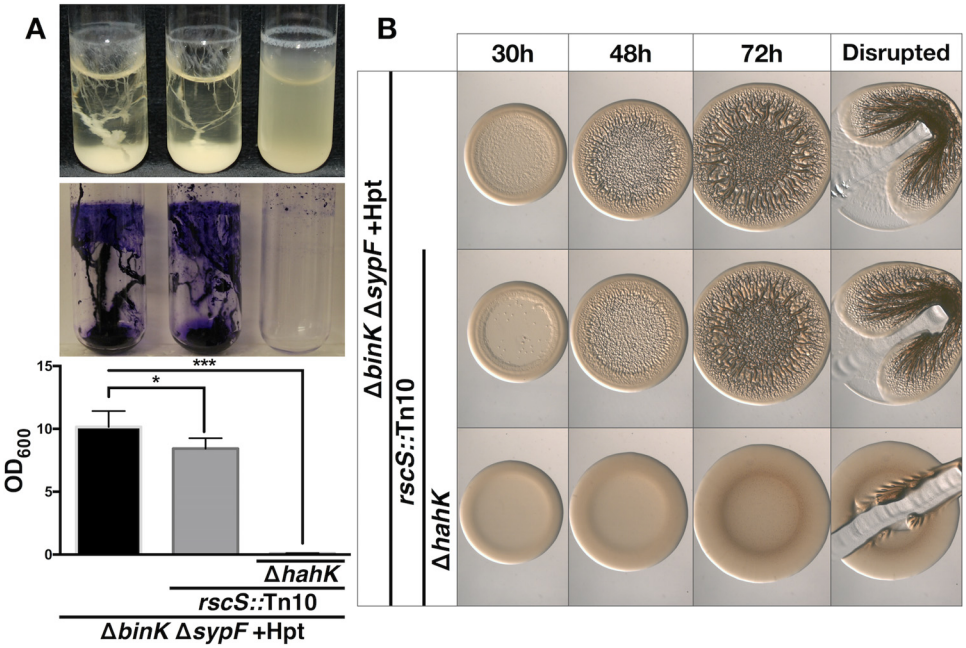

FIG 10 RscS contributes to calcium-dependent biofilms. The contributions of RscS and HahK to calcium-induced *V. fischeri* biofilms were evaluated using Δ*binK* Δ*sypF sypF-HPT* (KV7877), Δ*binK* Δ*sypF rscS*::Tn*10 sypF-HPT* (KV7949), and Δ*binK* Δ*sypF rscS*::Tn*10* Δ*hahK sypF-HPT* (KV8325) strains. (Top) Strains were grown shaking in LBS medium containing 10 mM $CaCl_2$ and imaged 16 h postinoculation. (Middle) Tubes were stained with crystal violet and imaged. (Bottom) Crystal violet was quantified, and a one-way ANOVA was performed (*P* values of 0.01 and 0.0009). (B) Wrinkled colony formation was assessed by incubation for 72 h on LBS agar plates supplemented with 10 mM $CaCl_2$. Colonies were disrupted to evaluate SYP-PS production.

readily form wrinkled colonies and pellicles in the absence of calcium. Although recent work had hinted at a role for calcium in these phenotypes, the impact of calcium was modest, presumably because biofilms were already quite robust (16). In contrast, RscS-overexpressing cells do not form biofilms when cells are grown in liquid cultures with shaking. Thus, it was with some surprise that we observed that calcium supplementation induced biofilm formation by RscS-overexpressing cells grown with shaking. Indeed, two distinct biofilm behaviors were noted, attachment to the surface at the air-liquid interface of shaking cultures (rings) and the production of a cohesive cellular clump (clumps). Because RscS-overexpressing cells do not normally form biofilms under these conditions in the absence of calcium, we conclude that calcium overcomes the regulatory processes that prevent biofilm formation by RscS-overexpressing cells under these conditions.

Calcium did not, however, permit SYP-PS-dependent biofilm formation by wild-type cells, indicating that multiple levels of control are in place. One such regulator turned out to be the negative regulator BinK, as calcium also induced the same phenotypes by a mutant defective only for BinK. In culture, the role of BinK as a negative regulator of biofilm formation had been previously established in the context of RscS overexpression; like calcium supplementation, disruption of *binK* only modestly increased wrinkled colony formation (33). Indeed, in the absence of calcium supplementation (or RscS overexpression), the *binK* mutant does not form biofilms. The addition of calcium, however, promoted all three biofilm phenotypes: wrinkled colony formation, pellicle production, and production of cohesive cellular clumps and rings. Together, these data further establish calcium as a powerful inducer of biofilm formation and reveal that a single regulator, BinK, is sufficient to prevent wild-type *V. fischeri* from responding to calcium to form biofilms.

Cohesive wrinkled colonies and pellicles are both dependent on SYP-PS (mutating *syp* genes fully disrupts both phenotypes). In contrast, disruption of SYP-PS production did not fully eliminate biofilms formed in calcium-supplemented shaking liquid cul-

tures. Instead, only clumps, but not rings, were disrupted by mutation of *syp*. This result provided new insight into these biofilms, permitting the identification of cellulose as a contributing factor responsible for ring formation. Understanding the specific contributions of the two polysaccharides will be an important future direction.

The discovery of conditions that promoted biofilm formation in the absence of overexpression of positive regulators permitted a reevaluation of the roles of known regulatory factors. Previous work using *rscS* overexpression indicated that RscS functioned upstream of the sensor kinase SypF (requiring only the Hpt domain of this protein) and the response regulator SypG. Similarly, SypF and SypG were required in the absence of BinK, suggesting that this pathway functions as previously determined using overexpression. However, the loss of RscS in a *binK* mutant did not significantly impact biofilm formation, even when only the Hpt domain of SypF was present. This finding indicated the involvement of another sensor kinase and led to the discovery that a previously uncharacterized regulator, HahK, also functions in biofilm formation. However, loss of HahK severely diminished, but did not eliminate, biofilm formation, suggesting the involvement of yet another sensor kinase; indeed, the remaining biofilm phenotypes were lost when *rscS* was also disrupted. These results are significant, as they (i) reveal HahK as a new biofilm regulator and (ii) identify, for the first time since it was identified in 2001 (39), a mutant phenotype in culture for *rscS*. We conclude that the activity of RscS is masked by redundancy with the activities of HahK and, potentially, SypF. The identification of conditions under which a phenotype for RscS can be observed in culture will permit additional studies designed to understand the signals and factors that control activity of RscS. Similarly, understanding the control over HahK activity, potentially via the nitric oxide sensor HnoX, encoded upstream (35, 36), is an important future direction.

Together, these findings reveal an increased complexity of the regulatory pathway controlling *syp*-dependent biofilm formation, with the involvement of four sensor kinases and two response regulators (Fig. 1). In other microbes, similarly complex pathways exist, e.g., *Vibrio lux* (40, 41), *Escherichia coli* Rcs (42, 43), *Pseudomonas* Roc (44), and Gac/RetS/Lad (45–49). For example, in *P. aeruginosa*, four sensor kinases feed into a pathway that controls, among other things, biofilm formation. The central regulator, the hybrid sensor kinase GacS, autophosphorylates and donates phosphoryl groups to the response regulator GacA, which controls the downstream events. In addition, the hybrid sensor kinase LadS feeds into the pathway by donating a phosphoryl group to the Hpt domain of GacS. Another hybrid sensor kinase, RetS, forms heterodimers that inhibit the activities of GacS and a fourth sensor kinase, PA1611. We envision that analogous events are happening with the Syp regulators. SypF is known to donate phosphoryl groups to SypG and SypE (26), yet its Hpt domain alone is sufficient for both biofilm formation in culture and symbiotic colonization, a result that validates our conclusions that other sensor kinases, presumably RscS and HahK, feed into the activation of SypF.

A lingering question is how calcium induces biofilm formation by *V. fischeri*. The answer to this question is unknown, although some specific mechanisms can be ruled out. For example, *V. fischeri* lacks the CarRS two-component system that, in *V. cholerae*, is induced in response to calcium and regulates transcription of the *Vibrio* polysaccharide locus *vps*. *V. fischeri* also lacks the *Vibrio vulnificus* calcium binding matrix protein CabA, which promotes biofilm formation in the latter organism (15). Further afield, *V. fischeri* also lacks the *Pseudomonas* sensor kinase LadS, which controls biofilm formation in response to calcium (50). Finally, it is unlikely that any of the known biofilm regulators function as a calcium sensor responsible for inducing biofilm formation: deletion of *sypF*, *rscS*, or *hahK* alone fails to prevent calcium-induced biofilm phenotypes. While SypF comes closest as a candidate for a calcium sensor, as the *sypF* mutant produces only cellulose-dependent biofilms in response to calcium, cell clumping is restored by just the Hpt domain of SypF, indicating that the sensory part of SypF is not necessary for this response. Similarly, while deletion of *binK* promotes biofilm formation, biofilms only form when calcium is added, a result that indicates the involvement

of another regulator. Thus, calcium may not be recognized by a two-component sensor in *V. fischeri*, and/or the response to calcium may be multifactorial. Future work will be directed at understanding how *V. fischeri* recognizes and responds to calcium.

In summary, this work has substantially advanced our understanding of the signals, pathways, and regulators that control biofilm formation by *V. fischeri*. It has established calcium as an important signal controlling the production of two different but interacting biofilms at the level of transcription. It has revealed conditions that promote biofilm formation in the absence of overexpressed regulators, permitting the discovery of a new regulator, HahK, that feeds into the control of biofilm formation, and the identification of a mutant phenotype for *rscS*. These conditions, and the knowledge gained here using them, will permit a mechanistic investigation of the signals and pathways involved in promoting biofilm formation in response to calcium.

MATERIALS AND METHODS

Strains and media. *V. fischeri* strains, plasmids, and primers used in this study are listed in Tables 1 and 2 and Table S1 in the supplemental material, respectively. All strains used in this study were derived from strain ES114, a bacterial isolate from *Euprymna scolopes* (51, 52). *V. fischeri* strains were grown in the complex medium LBS (53, 54). To induce biofilm formation, calcium chloride was added to a final concentration of 10 mM (or other concentrations, as indicated). Derivatives of *V. fischeri* were generated via conjugation, as previously described (55), or by natural transformation (56, 57). A variety of *E. coli* host strains, including GT115 (Invivogen, San Diego, CA), CC118 λ *pir* (58), TAM1 or TAM1 λ *pir* (Active Motif, Carlsbad, CA), DH5α (59), DH5α λ *pir* (60), Top10 F′ (Invitrogen, now Thermo Fisher Scientific), S17-1 λ *pir* (61), and π3813 (62), were used for the purposes of cloning, plasmid maintenance, and conjugation. *E. coli* strains were grown in LB (63). Solid media were made using agar to a final concentration of 1.5%. The following antibiotics were added to growth media as necessary, at the indicated final concentrations: chloramphenicol (Cm) at 1 μg ml^{-1} (*V. fischeri*) or 12.5 μg ml^{-1} (*E. coli*); erythromycin (Em) at 2.5 μg ml^{-1} (*V. fischeri*); tetracycline (Tc) at 5 μg ml^{-1} (*V. fischeri*) or 15 μg ml^{-1} (*E. coli*); ampicillin (Ap) at 100 μg ml^{-1} (*E. coli*); kanamycin (Km) at 100 μg ml^{-1} (*V. fischeri*) or 50 μg ml^{-1} (*E. coli*); and trimethoprim at 10 μg ml^{-1}. Along with any necessary antibiotics, thymidine was added to a final concentration of 0.3 mM for *E. coli* strain π3813.

Molecular techniques and strain construction. All plasmids were constructed using standard molecular biology techniques, with restriction and modification enzymes obtained from Thermo Fisher Scientific (Pittsburgh, PA). EMD Millipore Novagen KOD high-fidelity polymerase was used for PCR SOEing (splicing by overlap extension) (64) reactions, and Promega *Taq* was used to confirm gene deletion/insertion events. In some cases where PCR was used to generate DNA fragments, PCR cloning vector pJET1.2 (Fisher Scientific, Pittsburgh, PA) was used as an intermediate vector prior to cloning into the final vector. Unmarked deletions of *rscS* and *binK* were generated using pKV456 and pLL2, respectively, using an arabinose-inducible *ccdB* toxin approach as previously described (62, 65). For deletions of other genes, including *hahK* (*VF_A0072*), *VF1296*, *VF1053*, and *VF2379*, a PCR SOEing approach was used. Briefly, sequences (~500 bp) upstream and downstream of each gene were amplified by PCR. In addition, either an antibiotic resistance gene, along with flanking FRT sequences, was similarly amplified. The PCR primers used to generate the three DNA fragments (upstream sequence, antibiotic resistance marker, and downstream sequence) contained overlapping sequences that facilitated a SOEing reaction. Natural transformation was used to introduce the final spliced PCR product into *tfoX*-overexpressing *V. fischeri* strains (usually ES114), and the antibiotic resistance marker was used to select for the recombinant that contained the desired insertion/deletion mutation. Because natural transformation is more efficient using chromosomal DNA (56), chromosomal DNA was isolated from the recombinant strains using either the DNeasy blood and tissue kit (Qiagen) or the Quick-DNA Miniprep plus kit (Zymo Research) and used to introduce the desired mutation into additional strains. Insertion at the Tn*7* site of the chromosome was performed via tetraparental mating (66) between the *V. fischeri* recipient and three *E. coli* strains, carrying the conjugal plasmid pEVS104 (67), the Tn*7* transposase plasmid pUX-BF13 (68), and the pEVS107 derivative of interest. In some cases, sequences at or adjacent to the Tn*7* site or at other sites in the chromosome were introduced into *V. fischeri* strains via natural transformation and selection for the appropriate antibiotic resistance cassette. For example, the P*sypA-lacZ* reporter used here was positioned adjacent to the Tn*7* site. Either the empty Tn*7* cassette or the Tn*7* cassette containing one of several specific *sypF* alleles was subsequently introduced at the Tn*7* site of the P*sypA-lacZ* strain. Chromosomal DNA from the resulting strains was used to introduce the cassette and associated reporter into additional strains, such as those deleted for *hahK*, by selection for the Em^r cassette. In some cases, the antibiotic resistance cassette was removed from *V. fischeri* deletion/insertion mutants using Flp recombinase; this enzyme acts on FRT sequences to delete the intervening sequences, as has been shown previously (69).

Calcium-induced biofilm assay. To assess calcium-induced biofilm formation under shaking liquid conditions, LBS broth containing 10 mM calcium chloride was inoculated with single colonies of *V. fischeri* strains and grown overnight at 24°C with shaking. For these shaking liquid culture experiments, test tubes (13 by 100 mm) were used with a culture volume of 2 ml of LBS broth. Pictures are representative of at least 3 independent experiments. Photos were captured with either a Canon EOS Rebel T3i, Nikon D60, or iPhone 5 camera.

Crystal violet staining assay. Strains were grown in 2 ml LBS broth overnight, with 10 mM calcium chloride at 24°C as indicated. Two hundred microliters of a 1% crystal violet solution was added for 30 min. Tubes were washed with deionized H_2O, and liquid was removed via aspiration. Tubes were destained with ethanol, and the optical density at 600 nm (OD_{600}) was measured using a Synergy H1 microplate reader (BioTek). The data were compiled from at least three independent samples. Statistical analysis was performed using a one-way analysis of variance (ANOVA).

Wrinkled colony assay. *V. fischeri* strains were grown overnight at 28°C in LBS with antibiotics when necessary for plasmid maintenance. The overnight cultures were subcultured 1:100, grown until mid-log phase, and diluted to an OD_{600} of 0.2. Aliquots (10 μl) were spotted onto LBS agar supplemented with antibiotics or calcium chloride, as indicated. Spots were imaged at the indicated times, using consistent magnification with a Zeiss Stemi 2000-C dissecting microscope. At the final time point, the resulting colonies were disturbed with a toothpick to assess cohesiveness as a measure of SYP-PS production (38). Photos are representative of at least three independent experiments.

Pellicle assay. *V. fischeri* strains were grown overnight at 28°C in LBS medium. The overnight cultures were diluted to an OD_{600} of 0.2 in 2 ml of LBS medium supplemented with calcium chloride as indicated. Pellicles were incubated statically at 24°C and imaged at the indicated times, using consistent magnification, with a Zeiss Stemi 2000-C dissecting microscope. Pellicles were disturbed with a toothpick at the final time point to assess cohesiveness. Photos are representative of at least three independent experiments.

β-Galactosidase assay. Strains carrying a *lacZ* reporter fusion to the *sypA* promoter or to the *bcsQ* promoter were grown in triplicate at 24°C in LBS medium containing 10 mM calcium chloride. Strains were subcultured into 20 ml of fresh medium in 125-ml baffled flasks, the OD_{600} was measured and samples (1 ml) were collected after 22 h of growth. Cells were resuspended in Z-buffer and lysed with chloroform. The β-galactosidase activity of each sample was assayed as described previously (70) and measured using a Synergy H1 microplate reader (BioTek). The assay was performed at least three independent times. Statistical analysis was performed using a two-tailed *t* test.

SUPPLEMENTAL MATERIAL

Supplemental material for this article may be found at https://doi.org/10.1128/JB.00016-18.

SUPPLEMENTAL FILE 1, PDF file, 2.0 MB.

ACKNOWLEDGMENTS

We are grateful for insight gleaned from preliminary data of Anne Marsden and Valerie Ray. We thank Christine Bassis, Cindy Darnell, and Allison Norsworthy for strain construction, Randi Foxall and Cheryl Whistler for strains, and Jon Visick and members of the laboratory for thoughtful discussions and review of the manuscript.

This work was supported by NIH grant R01 GM114288, awarded to K.L.V.

REFERENCES

1. Branda SS, Vik S, Friedman L, Kolter R. 2005. Biofilms: the matrix revisited. Trends Microbiol 13:20–26. https://doi.org/10.1016/j.tim.2004.11.006.
2. Flemming HC, Wingender J. 2010. The biofilm matrix. Nat Rev Microbiol 8:623–633. https://doi.org/10.1038/nrmicro2415.
3. O'Toole G, Kaplan HB, Kolter R. 2000. Biofilm formation as microbial development. Annu Rev Microbiol 54:49–79. https://doi.org/10.1146/annurev.micro.54.1.49.
4. Watnick P, Kolter R. 2000. Biofilm, city of microbes. J Bacteriol 182:2675–2679. https://doi.org/10.1128/JB.182.10.2675-2679.2000.
5. Donlan RM. 2001. Biofilms and device-associated infections. Emerg Infect Dis 7:277–281. https://doi.org/10.3201/eid0702.010226.
6. Flemming HC, Neu TR, Wozniak DJ. 2007. The EPS matrix: the "house of biofilm cells." J Bacteriol 189:7945–7947.
7. Flemming HC, Wingender J, Szewzyk U, Steinberg P, Rice SA, Kjelleberg S. 2016. Biofilms: an emergent form of bacterial life. Nat Rev Microbiol 14:563–575. https://doi.org/10.1038/nrmicro.2016.94.
8. Arrizubieta MJ, Toledo-Arana A, Amorena B, Penades JR, Lasa I. 2004. Calcium inhibits Bap-dependent multicellular behavior in *Staphylococcus aureus*. J Bacteriol 186:7490–7498. https://doi.org/10.1128/JB.186.22.7490-7498.2004.
9. Bilecen K, Yildiz FH. 2009. Identification of a calcium-controlled negative regulatory system affecting *Vibrio cholerae* biofilm formation. Environ Microbiol 11:2015–2029. https://doi.org/10.1111/j.1462-2920.2009.01923.x.
10. Cruz LF, Cobine PA, De La Fuente L. 2012. Calcium increases *Xylella fastidiosa* surface attachment, biofilm formation, and twitching motility. Appl Environ Microbiol 78:1321–1331. https://doi.org/10.1128/AEM.06501-11.
11. Vozza NF, Abdian PL, Russo DM, Mongiardini EJ, Lodeiro AR, Molin S, Zorreguieta A. 2016. A *Rhizobium leguminosarum* CHDL (cadherin-like)-lectin participates in assembly and remodeling of the biofilm matrix. Front Microbiol 7:1608. https://doi.org/10.3389/fmicb.2016.01608.
12. Sarkisova S, Patrauchan MA, Berglund D, Nivens DE, Franklin MJ. 2005. Calcium-induced virulence factors associated with the extracellular matrix of mucoid *Pseudomonas aeruginosa* biofilms. J Bacteriol 187:4327–4337. https://doi.org/10.1128/JB.187.13.4327-4337.2005.
13. Garrison-Schilling KL, Grau BL, McCarter KS, Olivier BJ, Comeaux NE, Pettis GS. 2011. Calcium promotes exopolysaccharide phase variation and biofilm formation of the resulting phase variants in the human pathogen *Vibrio vulnificus*. Environ Microbiol 13:643–654. https://doi.org/10.1111/j.1462-2920.2010.02369.x.
14. Kierek K, Watnick PI. 2003. Environmental determinants of *Vibrio cholerae* biofilm development. Appl Environ Microbiol 69:5079–5088. https://doi.org/10.1128/AEM.69.9.5079-5088.2003.
15. Park JH, Jo Y, Jang SY, Kwon H, Irie Y, Parsek MR, Kim MH, Choi SH. 2015. The *cabABC* operon essential for biofilm and rugose colony development in *Vibrio vulnificus*. PLoS Pathog 11:e1005192. https://doi.org/10.1371/journal.ppat.1005192.
16. Marsden AE, Grudzinski K, Ondrey JM, DeLoney-Marino CR, Visick KL. 2017. Impact of salt and nutrient content on biofilm formation by *Vibrio fischeri*. PLoS One 12:e0169521. https://doi.org/10.1371/journal.pone.0169521.
17. McFall-Ngai MJ. 2014. The importance of microbes in animal

development: lessons from the squid-vibrio symbiosis. Annu Rev Microbiol 68:177–194. https://doi.org/10.1146/annurev-micro-091313-103654.
18. Stabb EV, Visick KL. 2013. *Vibrio fischeri*: a bioluminescent light-organ symbiont of the bobtail squid *Euprymna scolopes*, p 497–532. *In* Rosenberg E, DeLong EF, Stackebrand E, Lory S, Thompson F (ed), The prokaryotes, 4th ed. Springer-Verlag, Berlin, Germany.
19. Visick KL. 2009. An intricate network of regulators controls biofilm formation and colonization by *Vibrio fischeri*. Mol Microbiol 74:782–789. https://doi.org/10.1111/j.1365-2958.2009.06899.x.
20. Bassis CM, Visick KL. 2010. The cyclic-di-GMP phosphodiesterase BinA negatively regulates cellulose-containing biofilms in *Vibrio fischeri*. J Bacteriol 192:1269–1278. https://doi.org/10.1128/JB.01048-09.
21. Darnell CL, Hussa EA, Visick KL. 2008. The putative hybrid sensor kinase SypF coordinates biofilm formation in *Vibrio fischeri* by acting upstream of two response regulators, SypG and VpsR. J Bacteriol 190:4941–4950. https://doi.org/10.1128/JB.00197-08.
22. Yip ES, Geszvain K, DeLoney-Marino CR, Visick KL. 2006. The symbiosis regulator RscS controls the *syp* gene locus, biofilm formation and symbiotic aggregation by *Vibrio fischeri*. Mol Microbiol 62:1586–1600. https://doi.org/10.1111/j.1365-2958.2006.05475.x.
23. Shibata S, Yip ES, Quirke KP, Ondrey JM, Visick KL. 2012. Roles of the structural symbiosis polysaccharide (*syp*) genes in host colonization, biofilm formation and polysaccharide biosynthesis in *Vibrio fischeri*. J Bacteriol 194:6736–6747. https://doi.org/10.1128/JB.00707-12.
24. Yip ES, Grublesky BT, Hussa EA, Visick KL. 2005. A novel, conserved cluster of genes promotes symbiotic colonization and σ^{54}-dependent biofilm formation by *Vibrio fischeri*. Mol Microbiol 57:1485–1498. https://doi.org/10.1111/j.1365-2958.2005.04784.x.
25. Hussa EA, Darnell CL, Visick KL. 2008. RscS functions upstream of SypG to control the *syp* locus and biofilm formation in *Vibrio fischeri*. J Bacteriol 190:4576–4583. https://doi.org/10.1128/JB.00130-08.
26. Norsworthy AN, Visick KL. 2015. Signaling between two interacting sensor kinases promotes biofilms and colonization by a bacterial symbiont. Mol Microbiol 96:233–248. https://doi.org/10.1111/mmi.12932.
27. Morris AR, Darnell CL, Visick KL. 2011. Inactivation of a novel response regulator is necessary for biofilm formation and host colonization by *Vibrio fischeri*. Mol Microbiol 82:114–130. https://doi.org/10.1111/j.1365-2958.2011.07800.x.
28. Morris AR, Visick KL. 2013. The response regulator SypE controls biofilm formation and colonization through phosphorylation of the *syp*-encoded regulator SypA in *Vibrio fischeri*. Mol Microbiol 87:509–525. https://doi.org/10.1111/mmi.12109.
29. Ray VA, Eddy JL, Hussa EA, Misale M, Visick KL. 2013. The *syp* enhancer sequence plays a key role in transcriptional activation by the σ^{54}-dependent response regulator SypG and in biofilm formation and host colonization by *Vibrio fischeri*. J Bacteriol 195:5402–5412. https://doi.org/10.1128/JB.00689-13.
30. Groisman EA. 2016. Feedback control of two-component regulatory systems. Annu Rev Microbiol 70:103–124. https://doi.org/10.1146/annurev-micro-102215-095331.
31. Zschiedrich CP, Keidel V, Szurmant H. 2016. Molecular mechanisms of two-component signal transduction. J Mol Biol 428:3752–3775. https://doi.org/10.1016/j.jmb.2016.08.003.
32. Geszvain K, Visick KL. 2008. The hybrid sensor kinase RscS integrates positive and negative signals to modulate biofilm formation in *Vibrio fischeri*. J Bacteriol 190:4437–4446. https://doi.org/10.1128/JB.00055-08.
33. Brooks JF, Jr, Mandel MJ. 2016. The histidine kinase BinK is a negative regulator of biofilm formation and squid colonization. J Bacteriol 198:2596–2607. https://doi.org/10.1128/JB.00037-16.
34. Pankey MS, Foxall RL, Ster IM, Perry LA, Schuster BM, Donner RA, Coyle M, Cooper VS, Whistler CA. 2017. Host-selected mutations converging on a global regulator drive an adaptive leap by bacteria to symbiosis. Elife 6:e24414.
35. Nisbett LM, Boon EM. 2016. Nitric oxide regulation of H-NOX signaling pathways in bacteria. Biochemistry 55:4873–4884. https://doi.org/10.1021/acs.biochem.6b00754.
36. Wang Y, Dufour YS, Carlson HK, Donohue TJ, Marletta MA, Ruby EG. 2010. H-NOX-mediated nitric oxide sensing modulates symbiotic colonization by *Vibrio fischeri*. Proc Natl Acad Sci U S A 107:8375–8380. https://doi.org/10.1073/pnas.1003571107.
37. Nyholm SV, Stabb EV, Ruby EG, McFall-Ngai MJ. 2000. Establishment of an animal-bacterial association: recruiting symbiotic vibrios from the environment. Proc Natl Acad Sci U S A 97:10231–10235. https://doi.org/10.1073/pnas.97.18.10231.
38. Ray VA, Driks A, Visick KL. 2015. Identification of a novel matrix protein that promotes biofilm maturation in *Vibrio fischeri*. J Bacteriol 197:518–528. https://doi.org/10.1128/JB.02292-14.
39. Visick KL, Skoufos LM. 2001. Two-component sensor required for normal symbiotic colonization of *Euprymna scolopes* by *Vibrio fischeri*. J Bacteriol 183:835–842. https://doi.org/10.1128/JB.183.3.835-842.2001.
40. Henke JM, Bassler BL. 2004. Three parallel quorum-sensing systems regulate gene expression in *Vibrio harveyi*. J Bacteriol 186:6902–6914. https://doi.org/10.1128/JB.186.20.6902-6914.2004.
41. Miller MB, Skorupski K, Lenz DH, Taylor RK, Bassler BL. 2002. Parallel quorum sensing systems converge to regulate virulence in *Vibrio cholerae*. Cell 110:303–314. https://doi.org/10.1016/S0092-8674(02)00829-2.
42. Clarke DJ. 2010. The Rcs phosphorelay: more than just a two-component pathway. Future Microbiol 5:1173–1184. https://doi.org/10.2217/fmb.10.83.
43. Guo X-P, Sun Y-C. 2017. New insights into the non-orthodox two component Rcs phosphorelay system. Front Microbiol 8:2014. https://doi.org/10.3389/fmicb.2017.02014.
44. Sivaneson M, Mikkelsen H, Ventre I, Bordi C, Filloux A. 2011. Two-component regulatory systems in *Pseudomonas aeruginosa*: an intricate network mediating fimbrial and efflux pump gene expression. Mol Microbiol 79:1353–1366. https://doi.org/10.1111/j.1365-2958.2010.07527.x.
45. Bordi C, Lamy MC, Ventre I, Termine E, Hachani A, Fillet S, Roche B, Bleves S, Mejean V, Lazdunski A, Filloux A. 2010. Regulatory RNAs and the HptB/RetS signalling pathways fine-tune *Pseudomonas aeruginosa* pathogenesis. Mol Microbiol 76:1427–1443. https://doi.org/10.1111/j.1365-2958.2010.07146.x.
46. Goodman AL, Kulasekara B, Rietsch A, Boyd D, Smith RS, Lory S. 2004. A signaling network reciprocally regulates genes associated with acute infection and chronic persistence in *Pseudomonas aeruginosa*. Dev Cell 7:745–754. https://doi.org/10.1016/j.devcel.2004.08.020.
47. Goodman AL, Merighi M, Hyodo M, Ventre I, Filloux A, Lory S. 2009. Direct interaction between sensor kinase proteins mediates acute and chronic disease phenotypes in a bacterial pathogen. Genes Dev 23:249–259. https://doi.org/10.1101/gad.1739009.
48. Kong W, Chen L, Zhao J, Shen T, Surette MG, Shen L, Duan K. 2013. Hybrid sensor kinase PA1611 in *Pseudomonas aeruginosa* regulates transitions between acute and chronic infection through direct interaction with RetS. Mol Microbiol 88:784–797. https://doi.org/10.1111/mmi.12223.
49. Ventre I, Goodman AL, Vallet-Gely I, Vasseur P, Soscia C, Molin S, Bleves S, Lazdunski A, Lory S, Filloux A. 2006. Multiple sensors control reciprocal expression of *Pseudomonas aeruginosa* regulatory RNA and virulence genes. Proc Natl Acad Sci U S A 103:171–176. https://doi.org/10.1073/pnas.0507407103.
50. Broder UN, Jaeger T, Jenal U. 2016. LadS is a calcium-responsive kinase that induces acute-to-chronic virulence switch in *Pseudomonas aeruginosa*. Nat Microbiol 2:16184. https://doi.org/10.1038/nmicrobiol.2016.184.
51. Boettcher KJ, Ruby EG. 1990. Depressed light emission by symbiotic *Vibrio fischeri* of the sepiolid squid *Euprymna scolopes*. J Bacteriol 172:3701–3706. https://doi.org/10.1128/jb.172.7.3701-3706.1990.
52. Ruby EG, Urbanowski M, Campbell J, Dunn A, Faini M, Gunsalus R, Lostroh P, Lupp C, McCann J, Millikan D, Schaefer A, Stabb E, Stevens A, Visick K, Whistler C, Greenberg EP. 2005. Complete genome sequence of *Vibrio fischeri*: a symbiotic bacterium with pathogenic congeners. Proc Natl Acad Sci U S A 102:3004–3009. https://doi.org/10.1073/pnas.0409900102.
53. Graf J, Dunlap PV, Ruby EG. 1994. Effect of transposon-induced motility mutations on colonization of the host light organ by *Vibrio fischeri*. J Bacteriol 176:6986–6991. https://doi.org/10.1128/jb.176.22.6986-6991.1994.
54. Stabb EV, Reich KA, Ruby EG. 2001. *Vibrio fischeri* genes *hvnA* and *hvnB* encode secreted NAD(+)-glycohydrolases. J Bacteriol 183:309–317. https://doi.org/10.1128/JB.183.1.309-317.2001.
55. DeLoney CR, Bartley TM, Visick KL. 2002. Role for phosphoglucomutase in *Vibrio fischeri-Euprymna scolopes* symbiosis. J Bacteriol 184:5121–5129. https://doi.org/10.1128/JB.184.18.5121-5129.2002.
56. Pollack-Berti A, Wollenberg MS, Ruby EG. 2010. Natural transformation of *Vibrio fischeri* requires *tfoX* and *tfoY*. Environ Microbiol 12:2302–2311.
57. Brooks JF, Jr, Gyllborg MC, Cronin DC, Quillin SJ, Mallama CA, Foxall R, Whistler C, Goodman AL, Mandel MJ. 2014. Global discovery of coloni-

zation determinants in the squid symbiont *Vibrio fischeri*. Proc Natl Acad Sci U S A 111:17284–17289. https://doi.org/10.1073/pnas.1415957111.
58. Herrero M, de Lorenzo V, Timmis KN. 1990. Transposon vectors containing non-antibiotic resistance selection markers for cloning and stable chromosomal insertion of foreign genes in gram-negative bacteria. J Bacteriol 172:6557–6567. https://doi.org/10.1128/jb.172.11.6557-6567.1990.
59. Hanahan D. 1983. Studies on transformation of *Escherichia coli* with plasmids. J Mol Biol 166:557–580. https://doi.org/10.1016/S0022-2836(83)80284-8.
60. Dunn AK, Martin MO, Stabb E. 2005. Characterization of pES213, a small mobilizable plasmid from *Vibrio fischeri*. Plasmid 54:114–134. https://doi.org/10.1016/j.plasmid.2005.01.003.
61. Simon R, Priefer U, Puhler A. 1983. A broad host range mobilization system for *in vivo* genetic engineering: transposon mutagenesis in gram negative bacteria. Bio/Technol 1:784–791. https://doi.org/10.1038/nbt1183-784.
62. Le Roux F, Binesse J, Saulnier D, Mazel D. 2007. Construction of a *Vibrio splendidus* mutant lacking the metalloprotease gene *vsm* by use of a novel counterselectable suicide vector. Appl Environ Microbiol 73:777–784.
63. Davis RW, Botstein D, Roth JR. 1980. Advanced bacterial genetics. Cold Spring Harbor Laboratory, Cold Spring Harbor, NY.
64. Ho SN, Hunt HD, Horton RM, Pullen JK, Pease LR. 1989. Site-directed mutagenesis by overlap extension using the polymerase chain reaction. Gene 77:51–59.
65. Shibata S, Visick KL. 2012. Sensor kinase RscS induces the production of antigenically distinct outer membrane vesicles that depend on the symbiosis polysaccharide locus in *Vibrio fischeri*. J Bacteriol 194:185–194. https://doi.org/10.1128/JB.05926-11.
66. McCann J, Stabb EV, Millikan DS, Ruby EG. 2003. Population dynamics of *Vibrio fischeri* during infection of *Euprymna scolopes*. Appl Environ Microbiol 69:5928–5934. https://doi.org/10.1128/AEM.69.10.5928-5934.2003.
67. Stabb EV, Ruby EG. 2002. RP4-based plasmids for conjugation between *Escherichia coli* and members of the *Vibrionaceae*. Methods Enzymol 358:413–426. https://doi.org/10.1016/S0076-6879(02)58106-4.
68. Bao Y, Lies DP, Fu H, Roberts GP. 1991. An improved Tn*7*-based system for the single-copy insertion of cloned genes into chromosomes of Gram-negative bacteria. Gene 109:167–168. https://doi.org/10.1016/0378-1119(91)90604-A.
69. Cherepanov PP, Wackernagel W. 1995. Gene disruption in *Escherichia coli*: TcR and KmR cassettes with the option of Flp-catalyzed excision of the antibiotic-resistance determinant. Gene 158:9–14.
70. Miller JH. 1972. Experiments in molecular genetics. Cold Spring Harbor Laboratory, New York, NY.
71. Hussa EA, O'Shea TM, Darnell CL, Ruby EG, Visick KL. 2007. Two-component response regulators of *Vibrio fischeri*: identification, mutagenesis, and characterization. J Bacteriol 189:5825–5838. https://doi.org/10.1128/JB.00242-07.
72. Visick KL, Quirke KP, McEwen SM. 2013. Arabinose induces pellicle formation by *Vibrio fischeri*. Appl Environ Microbiol 79:2069–2080. https://doi.org/10.1128/AEM.03526-12.
73. Ondrey JM, Visick KL. 2014. Engineering *Vibrio fischeri* for inducible gene expression. Open Microbiol J 8:122–129. https://doi.org/10.2174/1874285801408010122.